Study of Hydroelastic Effects on Sloshing Flows due to Flexible Baffle

Taehyun Park, Cheon-Jin Park, Jeoungkyu Lee, and Yonghwan Kim
Department of Naval Architecture and Ocean Engineering,
Seoul National University, Seoul, Korea
thth0325@snu.ac.kr

1 INTRODUCTION

The sloshing phenomenon, a free-surface flow that occurs in partially-filled liquid cargo containers, is observed in various fields, such as ship cargo and fuel tanks. It is important to understand the interaction between the sloshing flow and the structure because sloshing can have a structural impact on the container. Over the past decades, interest has increased in solving the fluid-structure interaction (FSI) problem with a free surface. With the rapid growth of computing, numerical analysis methods have developed, and there have been experiments on representative cases to be used as reference data for numerical analysis [1]. Since then, there have been studies comparing the results of [1] with the results of various numerical FSI analysis methods [2-4], but few studies have systematically verified them experimentally.

This study conducted sloshing experiments in a rectangular tank with internal baffles. Experimental results were compared on a flexible baffle, a rigid baffle, and without baffles. Various experiments were conducted for different filling levels, amplitude, and frequency in order to observe the hydroelasticity effects of internal baffles on sloshing flows. In this abstract, some experimental and numerical results of FSI are shown, and eventually, it is planned to open our measured data to the public domain.

2 TEST OVERVIEWS

2.1 Experimental Setup

The model experiments were carried out at the Sloshing Experimental Facility of Seoul National University (SNU). A 2D acrylic model tank was mounted on a 6-DoF motion platform with a 1.5-ton capacity (Fig.1). The rectangular tank is 1 m long, 8 cm wide, and 60 cm high. Plate-shaped internal baffles were fixed to the center of the tank bottom using aluminum blocks. The baffle size is 10 cm in height, 8 cm in width, and 4 mm in thickness. Two types of internal baffles were used; a flexible baffle made of nitrile butadiene rubber (NBR) and a rigid baffle made of brass. The density of the flexible baffle is 1.26 g/cm^3, and the stress-strain curve of the flexible baffle used in the experiment is shown in Fig. 1. In this experiment, regular sway motions for about 500 cycles were applied.

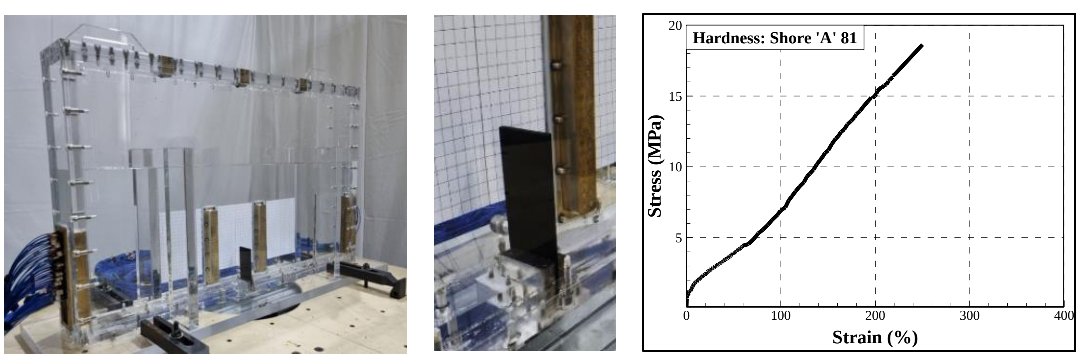

Figure 1: Experiment tank (left), baffle (middle), and the stress-strain curve of flexible baffle (right)

2.2 Measurement System

Sloshing pressures were measured with Integrated Circuit Piezoelectric (ICP) type dynamic pressure sensors (211B5 from KISTLER Co.). A total of 160 sensors were arranged in the side and back faces of the tank. The sampling frequency was fixed at 20 kHz, and the pressure threshold used for the Peak-over threshold method was 2.5 kPa. PIV measurement was carried out to observe the fluid flows around the baffles. To this end, a Y4-S2 high-speed camera of Integrated Design Tools mounted in the front of the model tank, captured 1,000 photos per second.

2.3 Fluid-structure Interaction Analysis

The FSI analysis technique is divided mainly into the direct coupling scheme and the partitioned coupling scheme (partitioned method). In this study, the partitioned method which solves for each fluid and solid domain and exchanges data at the fluid-structure boundary is applied. ABAQUS was applied for the FSI analysis, and a user-defined function was adopted for the interaction of fluid and baffle.

3 RESULTS

3.1 Free-surface Flow around Internal Baffles

Examples of free-surface flows around the rigid and flexible internal baffles are shown in Fig. 2. The filling level is 20% of the tank height close to the tip of the internal baffle, and the motion frequency is the natural frequency of the tank without the baffle. The solid lines are the wave elevations of each case. As the flexible baffle bends, the flow passing over the baffle combines with the flow generated by the movement of the baffle and moves further. The wave slope around the rigid baffle is steeper, and the locations of the lowest elevation are different.

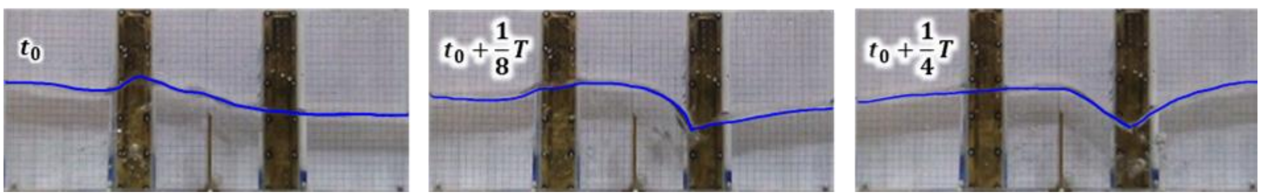

(a) Rigid baffle

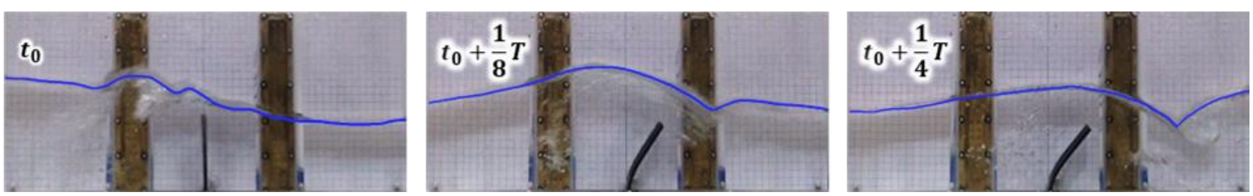

(b) Flexible baffle

Figure 2: Free-surface flow profiles around internal baffles: 20% filling, 5 cm sway amplitude(A), 3.7824 rad/sec sway frequency(ω)

3.2 Maximum Displacement of Flexible Baffle

The measured maximum displacements of the internal flexible baffle for different test conditions are compared in Fig. 3. The maximum displacement was measured at the tip of the flexible baffle. The experimental results were for three filling levels, 20%, 40%, and 60%. The motion amplitude was discretized into 3, 5, and 7 cm, and the motion frequency varied from 0.5 to 2.0 times of the natural frequency of the no-baffle case. The maximum displacement results are shown in Fig. 3. The displacement is normalized by the height of the baffle as δ/H where δ is the displacement, and H is the height of the baffle. Naturally, the displacement increases as the motion amplitude increases. It is interesting that the displacement doesn't change much at 20% filling and high-frequency excitations. As the filling level increases, the maximum displacement occurs near the natural frequency of the tank without a baffle. It can be easily understood that the natural frequency shifts higher frequency as the filling height is closer to the baffle height, and the baffle effect becomes stronger.

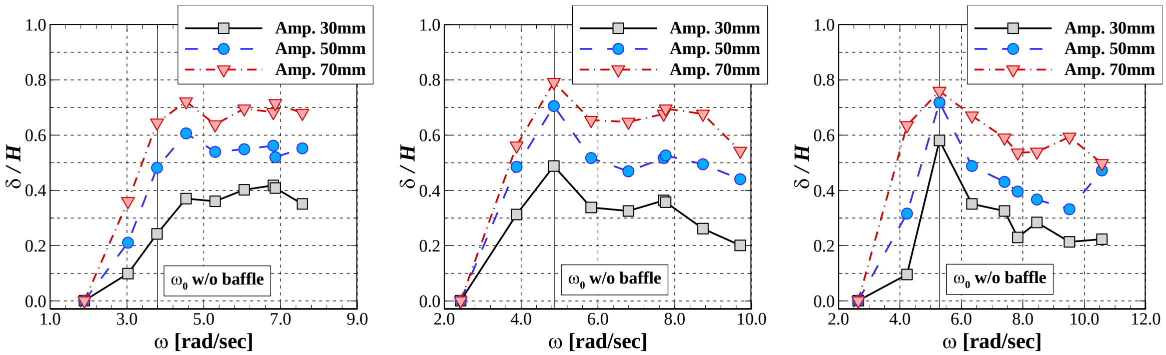

(a) 20% filling (b) 40% filling (c) 60% filling

Figure 3: Maximum displacement of the flexible baffle

3.3 PIV Measurement of Fluid Flow

PIV measurement is a good technique for observing detailed flows, but it is not easy to measure sloshing flows. It is partly due to the unsteadiness and nonlinearity of sloshing flows, and also there are some difficulties in capturing clean shots by a high-speed camera. For example, an acryl wall has many reflections of laser light, and it prevents making good photographs of particles. Fig. 4 shows four photos with velocity vectors at 60% filling and their time interval is 0.03 sec. In this case, the motion amplitude is large (7 cm), and the displacement of the flexible baffle is large. It is obvious that the deformation of the baffle and vortex generation have an interaction. As the deformation becomes large, the faster velocity over the baffle and stronger vortex generation can be shown, and the vortex is moving away from the baffle. The detailed observation will be explained in the workshop.

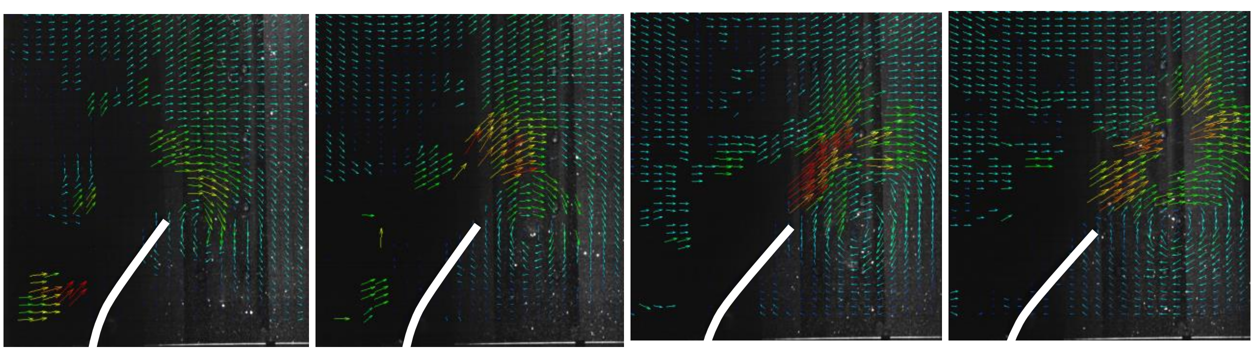

Figure 4: Example of PIV measurement: 60%H filling, 7 cm, and 5.286 rad/sec excitation

3.4 Comparison of the Average of 10 Largest Peak Pressures

The measured pressures at the 20% filling which has the most significant influence on the internal baffle are shown in Fig. 5. In this case, the motion amplitude is 5 cm. The results of the case without baffle are compared to observe how much different the peak pressures are. The pressure (P) in Fig. 4 is normalized with respect to the density of the fluid (ρ), gravitational acceleration (g), and the tank length (L), i.e. $P/\rho g L$. Without an internal baffle, sloshing impact occurred mostly on the side panel under conditions near the natural frequency, and slightly high pressures were also observed on the wall around the baffle. When the rigid baffle was positioned, the sloshing-induced impact did not occur on both sides at low frequencies, but gradually occurred as the motion frequency became high. When the flexible baffle was equipped, the flow was disturbed by the elasticity of the baffle, resulting in a complex flow. Energy is consumed by the deformation of the baffle's shape, reducing the pressure measured from the side panel.

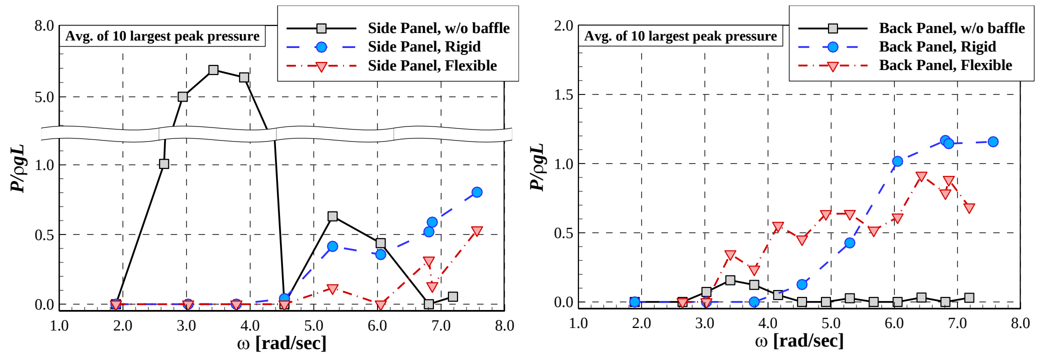

(a) Side wall (b) Back wall

Figure 5: Average of 10 largest peak pressures for different baffles: 20%filling, 5 cm sway excitation

3.5 Numerical Analysis of Fluid-Structure Interaction

Fig. 6 shows an example of a numerical solution of the 2-way coupling FSI analysis. The numerical solutions can be compared for the deformation profile and maximum displacement of the baffle, free surface profile, and hydrodynamic pressure. The details will be introduced in the workshop.

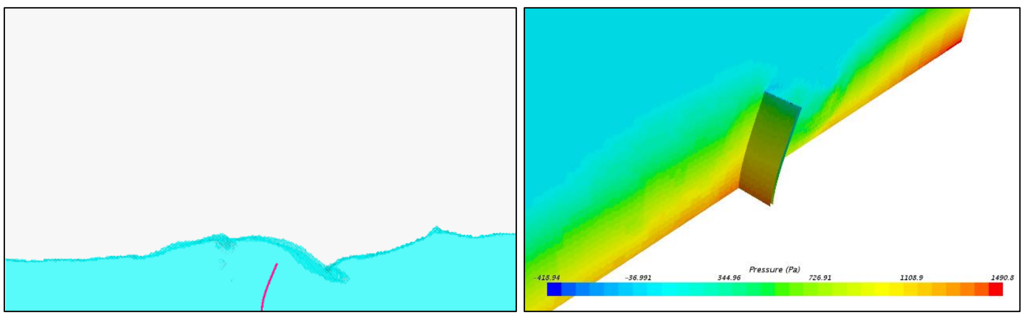

Figure 6: Example results of numerical FSI analysis using 2-way coupling

4 CONCLUSIONS

A series of experiments have been presented to determine the relationship between the properties of the baffle and wave condition when there was an internal baffle in the sloshing flow. If the baffle is flexible, the free surface wave becomes more nonlinear, and the vortex occurs significantly. These experimental results can be compared with numerical FSI analysis results for various perspectives.

REFERENCES

[1] Idelsohn, S. R., Marti, J., Souto-Iglesias, A., & Oñate, E. (2008). Interaction between an elastic structure and free-surface flows experimental versus numerical comparisons using the PFEM. Computational Mechanics, 43(1), 125-132

[2] Degroote, J., Souto-Iglesias, A., Van Paepegem, W., Annerel, S., Bruggeman, P., & Vierendeels, J. (2010). Partitioned simulation of the interaction between an elastic structure and free surface flow. Computer methods in applied mechanics and engineering, 199(33-36), 2085-2098.

[3] Hwang, S. C., Park, J. C., Gotoh, H., Khayyer, A., & Kang, K. J. (2016). Numerical simulations of sloshing flow with elastic baffles by using a particle-based fluid-structure interaction analysis method. Ocean Engineering, 118, 227-241.

[4] Zhang, Z. L., Khalid, M. S. U., Long, T., Chang, J. Z., & Liu, M. B. (2020). Investigations on sloshing mitigation using elastic baffles by coupling smoothed finite element method and decoupled finite particle method. Journal of Fluids and Structures, 94, 102942.